Reaction Dynamics in Acidic Zeolites: Room Temperature Tunneling Effects

Justin T. Fermann[a] and Scott M. Auerbach[a,b,*]

[a]Department of Chemistry, University of Massachusetts, Amherst, MA 01003

[b]Department of Chemical Engineering, University of Massachusetts, Amherst, MA 01003

We present recommendations for accurately and efficiently calculating transition state parameters for proton transfer reactions in zeolites. Density functional theory with the B3LYP functional is sufficient for obtaining accurate structures and vibrational frequencies. MP2 energies in larger basis sets augmented with MP4 energies in more limited basis sets yield accurate classical barrier heights. Even after applying a correction for the effect of long range interactions, the barrier heights we calculate are significantly larger than those reported in the experimental literature. By evaluating temperature dependent proton transfer rate constants using both the harmonic and sudden limits of semiclassical transition state theory, we attribute the discrepancy to the neglect of tunneling in the interpretation of experimental data.

1. Introduction

To better understand and design zeolite catalysts,[1, 2] it is imperative that we have a detailed and accurate concept of the elementary steps that make up complex catalysis reaction pathways. Although there is a vast amount of experimental data on zeolite catalyzed reactions, in most cases the reaction mechanisms themselves are incompletely understood. Often such understanding cannot be obtained solely from the experiments we can perform currently; theoretical investigations of these reactions offer an important, complementary glimpse into the microscopic reaction dynamics governing these processes.[2–5] Our primary goal is to demonstrate a means of calculating temperature dependent elementary reaction rate coefficients for proton transfer in bare zeolites. We focus on a prototypical proton transfer reaction, from O(1) to O(4) in H–Y zeolite, in order to compare our results with an experimental determination of the activation energy.[6] In this work we study relatively small clusters and apply simple quantum rate theories. We summarize our results to date, establishing reasonable convergence of electronic structure calculations and demonstrating the importance of tunneling at ambient temperatures by applying our rate theory using the results of those calculations.

In Section 2.1, we describe the cluster model of H–Y zeolite and the electronic structure methods we use to compute classical barrier heights with "chemical accuracy," approximately 10 kJ mol^{-1}, for the given zeolite model.[7] Sauer and coworkers have analyzed

---

[*] Corresponding author; email: `auerbach@chem.umass.edu`

the effect of long–range electrostatic forces using their embedded cluster methodology, and their results give us an estimate of how these affect classical barrier heights.[8, 9] In Section 2.2, we present the formulations of stabilized semiclassical transition state theory [SC–TST] we use to compute rate coefficients.[10, 11]

In Section 3, we present our best description of the proton transfer potential energy surface [PES] from the electronic structure calculations. The barrier heights we calculate, even correcting for long range interactions, are significantly larger than those reported in the experimental literature.[6] It is possible that this apparent discrepancy is a result of water or other impurities providing alternate reaction pathways with substantially lower activation energies.[5, 12] We explore instead the possibility that quantum mechanical tunneling plays a significant role in the dynamics even at ambient temperatures. We use our best PES data to apply the forms of SC–TST, obtaining rate coefficients over a broad range of temperatures.[7, 11] We find that for the proton transfer reaction studied here, our results indicate that quantum mechanical tunneling is the dominant mechanism up to and slightly above room temperature.

2. Methods

2.1. Rate Theory Parameters from Electronic Structure Theory

To parameterize the rate theories in Section 2.2 using electronic structure theory, we must compute the energies and full sets of harmonic vibrational frequencies at a selected set of points on the PES. Although there has been much recent work on various embedding techniques because long range interactions are an important component of accurate energetics,[9, 13] we focus on cluster models here for convenience in showing convergence of *ab initio* results. Our conclusions directly impact the choice of electronic structure theory used in embedded cluster and periodic calculations. In this work, we establish convergence of the electronic structure calculations, and use results from other work[8, 9] to include long range effects in an approximate fashion.

From our initial convergence studies,[7] we concluded that the B3LYP[14, 15] density functional with polarized basis sets of triple–ζ quality in the valence is adequate and efficient for calculating structures and harmonic vibrational frequencies with error bars of ca. 200 cm^{-1}, but fails to give quantitative energy differences. For converging properties such as the classical barrier height to 10 kJ mol^{-1}, we augment MP2[16] single point energies in a larger basis set with MP4[17, 18]/MP2 energy differences in a smaller basis. To then parameterize the rate theories, this technique was applied using a reasonable cluster model of a zeolite with $\mathrm{H_3Si\underline{O}Al(OH)_2\underline{O}SiH_3^-/H^+}$ stoichiometry.[3–5, 7, 8, 19] The underlined oxygens are the donor and acceptor in the proton transfer, O(1) and O(4). Initial geometric parameters were taken from neutron diffraction experiments.[20] The terminal hydrogens of this species were mechanically constrained to reproduce the covalent footprint of the cavity in H–Y zeolite from which the cluster is “clipped.”

Stationary points were located along the minimum energy path using analytic gradient techniques.[21–23] Transition structures were found using mode following algorithms in the proton transfer reaction coordinate.[21] Harmonic vibrational frequencies were evaluated by normal mode analysis of the mass weighted Hessian.[22, 24, 25] To remove spurious vibrational frequencies and complete the mechanical embedding of the cluster, the mass of each terminal atom (H) was set to a large number, e.g. 10^6 au, in the normal mode analysis. Single point energies were computed at higher correlated levels of theory. This completes the parameterization of conventional SC–TST.

To parameterize the sudden approximation of SC–TST, more extensive data were required. Points were located by geometrically constrained optimization or mode following at a series of eight fixed O–Al–O angles ranging from 76° to 94°, spanning the reactant minimum and the transition state angle. At the relevant points, electronic energies and vibrational frequencies were obtained as above. For computational efficiency, only the B3LYP density functional method was used to parameterize the sudden SC–TST. This underestimated the classical barrier by approximately 10 kJ mol^{-1}, but allowed us to make quantitative comparisons between the two rate theories we advocate below. All electronic structure calculations were performed using the GAUSSIAN98 suite[26] or PSI suite[27] of quantum chemistry programs.

2.2. Semiclassical Rate Theory

The rate theories we use to compute temperature dependent rate coefficients, $k(T)$, evolve from the semiclassical transition state theory of Hernandez and Miller.[28, 29] Here we give only our working formulae; for a complete derivation of these rate expressions, see references [10] and [11].

Adiabatic Limit

Miller and coworkers originally extended one dimensional tunneling theory to multidimensional cases of chemical interest by introducing a generalized barrier penetration integral, θ.[28–30] Enforcing harmonic, and therefore separable, dynamics results in purely harmonic quantum transition state theory, which is known to known to diverge at or below the temperature $T^* \equiv \hbar|\omega_F^\ddagger|/2\pi k_B$. Here $|\omega_F^\ddagger|$ is the magnitude of the imaginary vibrational frequency of the reaction coordinate, q_F, at the transition state, $h = 2\pi\hbar$ is Planck's constant, and k_B is Boltzmann's constant. T^* is 360 K for the system we studied, with $|\overline{\nu}_F^\ddagger| = |\omega_F^\ddagger|/2\pi c = 1570$ cm^{-1} (c is the speed of light).[7] Because many zeolite experiments are performed at or below 360 K, it is important to have a rate theory that extends into the deeper tunneling regime. Associating a maximum value of θ with the zero point vibrational energy [ZPVE] corrected ground state of the reactants, we derived a rate expression that smoothly connects deep tunneling theory[31] with the high temperature limit of purely harmonic SC–TST, according to:[10]

$$k(T) = k^{\mathrm{TST}}(T) \cdot \Gamma(T) \tag{1}$$

$$k^{\mathrm{TST}}(T) = \frac{k_B T}{h} \frac{Q^\ddagger}{Q^r} \tag{2}$$

$$\Gamma(T) = \frac{e^{\beta \Delta E_0}}{1 + e^{2\theta_0}} + \frac{1}{2} \int_{-\infty}^{\theta_0} d\theta e^{\beta \Delta E_0 \theta / \theta_0} \mathrm{sech}^2 \theta \tag{3}$$

Here, Q^r is the partition function at the reactant minimum; $Q^\ddagger$ is the partition function at the transition state; ΔE_0 is the ZPVE corrected classical barrier height; and $\beta = 1/k_B T$. The partition functions, Q, and barrier height, ΔE_0, are specified by the electronic energies and vibrational frequencies at the reactant and transition state, and $\theta_0 = \pi \Delta E_0/\hbar|\omega_F^\ddagger|$. These parameters are obtained from the electronic structure calculations described in Section 2.1. The tunneling correction factor, $\Gamma(T)$, is then evaluated numerically. The principal assumptions we make in deriving Eqs. 1–3 are that dynamics are confined to the minimum energy path [MEP], the barrier is always parabolic, and the energy can be written as a separable function of normal mode coordinates. We will address issues of barrier anharmonicity in a future publication, and issues of reaction path curvature, or "corner cutting," with the sudden approximation below.

Sudden Limit

In harmonic SC–TST the focus is on the flux through the transition state, and the dynamics are governed by the MEP. This tacitly assumes that the zeolite framework equilibrates to the motion of the proton, but the small mass of hydrogen makes it more likely that the proton hop is rapid compared to relaxation of the zeolite framework. In effect, we now take the thermal motions of the zeolite framework to modulate the height and width of the barrier that the proton must cross. The local degree of freedom that couples most strongly with the proton hopping reaction coordinate is the O–Al–O angle, which changes by 15° along the MEP. A sudden approximation entails performing fixed–angle rate calculations at a series of O–Al–O angles encompassing both the reactant angle, ϕ^r, and the transition state angle, $\phi^\ddagger$. These individual fixed–angle rate coefficients are averaged with proper weighting, giving:

$$k(T) \cong \int d\phi \rho(\phi, T) k(\phi, T) \cong \sum_{j=1}^{N_\phi} \Delta\phi_j \rho(\phi_j, T) k(\phi_j, T). \tag{4}$$

Here, $k(\phi_j, T)$ is the fixed–angle rate coefficient calculated using Eqs. 1–3 with parameters from geometrically constrained *ab initio* calculations. $\rho(\phi_j, T)$ is then the Boltzmann weight of the reactant state at angle ϕ_j with energy $V^r(\phi_j)$,

$$\rho(\phi_j, T) = e^{-\beta V^r(\phi_j)} / \sum_{j'=1}^{N_\phi} e^{-\beta V^r(\phi'_j)}. \tag{5}$$

This is the relative probability that classical energetic fluctuations in the zeolite framework at temperature T will cause the O–Al–O angle to assume the value ϕ_j; thus ρ decreases away from the reactant angle.

3. Results and Discussion

Adiabatic Approximation

Parameterization of the adiabatic SC–TST resulted in the MEP depicted in Fig. 1. Our original data from reference [7] are partly reproduced in Table 1. We observe that MP2 and B3LYP give roughly identical vibrational data, but the DFT method is far less computationally expensive. Only MP2 and MP4 reproduce the high–level CCSD(T)[32, 33] results to within a few kJ mol^{-1}. The difference $E(\text{MP4}) - E(\text{MP2})$ is roughly constant with respect to basis set, 0.6 to 1.1 kJ mol^{-1}, justifying the calculation technique outlined in Section 2.1. Using the results of Sauer and coworkers,[8] we estimate that long range interactions increase the barrier height by approximately 11 kJ mol^{-1}. Adding this to our most reliable result (86.1 kJ mol^{-1}) gives our best estimate of the activation energy along the MEP, 97.1 $\pm$ 10 kJ mol^{-1}. Using this value of ΔE_0 and $|\overline{\nu}_F^\ddagger| = 1570 \pm 200$ cm^{-1}, we apply our SC–TST to construct Fig. 2. This Arrhenius plot encapsulates our elementary understanding of the proton transfer process.

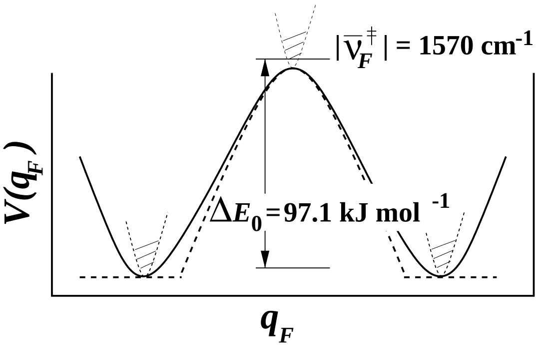

Figure 1. Minimum energy path obtained by highest level electronic structure calculations, q_F is the reaction coordinate.

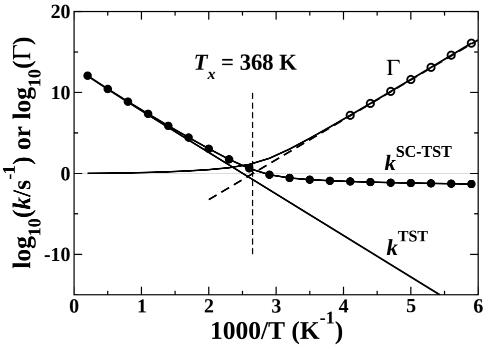

Figure 2. Arrhenius plot from adiabatic rate equation with geometric definition of T_x, the tunneling transition temperature.

The semiclassical rate follows the TST rate in the high temperature region of Fig. 2. At low temperatures, the temperature dependence of $k^{\mathrm{SC-TST}}(T)$ becomes very weak, as expected from experiment and theory.[34] The point where the two approximately linear sections would hypothetically intersect is labeled T_x, the tunneling crossover temperature. In a rough sense, at temperatures above T_x, tunneling is negligible, but below T_x tunneling is dominant. This crossover temperature is 368 ± 48 K given the above parameters. Virtually all of the uncertainty in T_x comes from the error bounds we place on $|\overline{\nu}^{\ddagger}_F|$, because T_x is a stronger function of the barrier width as long as $\Delta E_0 \gg hc|\overline{\nu}^{\ddagger}_F|$. It is interesting to note that under these conditions, T_x is closely approximated by $T^* \equiv \hbar|\omega^{\ddagger}_F|/2\pi k_B$, the harmonic divergence temperature.[10] This offers a reasonable estimation of the temperature regime of traditional transition state theory, and when experiments are performed near or below this temperature it will be imperative to include some account of tunneling in the interpretation of measurements.

To see this further, we compare the classical barrier height we predict above with the activation energy extracted from temperature dependent MAS–NMR measurements. Sarv and coworkers analyzed spinning side band intensities at four temperatures (298 K, 478 K, 568 K, 658 K) and deduced an activation energy for proton rearrangement in H–Y zeolite of 61 kJ mol^{-1}.[6] This is in clear disagreement with the 97.1 kJ mol^{-1} barrier we compute. However, by *forcing* an Arrhenius fit through our calculated rate coefficients at four corresponding points, which clearly exhibit non–Arrhenius behavior, we obtain an *apparent* activation energy of 60.3 kJ mol^{-1}. This agreement must be partially fortuitous, but it does illustrate that classical barrier heights could be severely underestimated if tunneling is neglected in the interpretation of experimental rate data. To extract proton transfer barrier heights, it will be necessary to perform experiments over a wider range and finer mesh of temperatures, and perhaps fit the results to a form such as

$$\log_{10}[k(T)] = \log_{10}[Ae^{-E_a/k_BT} + k^{\mathrm{tunneling}}]. \tag{6}$$

Isotopically substituting deuterium for the proton decreases the curvature of the barrier by ca. $1/\sqrt{2}$, and correspondingly diminishes the importance of tunneling for the $^2\mathrm{H}^+$ hop.

Table 1
Summary of electronic structure results for 3T cluster. Energies in kJ mol^{-1}. Reproduced from Reference [7].

Basis set [NBF$^{a)}$]	Level of theory	ΔV_0	Δ ZPVE	ΔE_0	$\lvert\overline{\nu}_F^\ddagger\rvert$ (cm^{-1})
6–31G(d)[135]	HF	144.5	−14.2	130.3	2009.7
	BLYP	67.7	−13.6	54.1	1345.7
	B3LYP	85.0	−13.7	71.2	1512.1
	MP2	92.0	−13.6	78.4	1570.2
	MP4^b	93.1	–	79.5	–
	CCSD(T)^b	94.9	–	81.3	–
6–311G(d,p)[204]	HF	150.2	−14.7	135.4	2004.7
	BLYP	72.8	−13.6	59.2	1374.5
	B3LYP	90.2	−13.9	76.3	1528.1
	MP2^b	99.1	–	85.5	–
	MP4^b	99.7	–	86.1	–

a) Number of basis functions.
b) Using MP2/6–31G(d) frequencies.

For D–Y zeolite, we find that $T_x = 264$ K. We expect that measurements of jump rates for deuterated zeolites at room temperature and above will yield reasonable values for classical barrier heights.

Sudden Approximation

To allow for multiple reaction paths *via* a weighted average of fixed–angle jump rates, we calculate dynamical parameters for eight fixed O–Al–O angles as described in the Section 2.1. Three of those fixed–angle paths are shown schematically in Fig. 3. We observe that both barrier height and curvature increase as the O–Al–O angle changes from $\phi^\ddagger \cong 76.64^{\text{o}}$ to $\phi^r = 93.64^{\text{o}}$. The relationship between the frozen local coordinate, ϕ, and the reaction coordinate, q_F, are depicted in the contour diagram inset in Fig. 3. The fixed–angle activation energies, as well $|\omega_F^\ddagger|$ at the fixed–angle transition state, both increase away from the first order saddle point in such a way that $k(\phi)$ increases from ϕ^r to $\phi^\ddagger$. The product $\rho(\phi)k(\phi)$ exhibits a peak between ϕ^r and $\phi^\ddagger$, indicating that there is a dynamical distribution of paths contributing to the overall rate, in accord with so–called large curvature dynamics. This peak is broader at higher temperatures, and at high enough temperatures the dynamical distribution flattens out to easily encompass the saddle point region, validating the use of techniques that focus on the minimum energy path.

In Fig. 4 we compare the results from the adiabatic approximation and the sudden approximation, both evaluated using parameters from the B3LYP/6-311G(d,p) level of theory. There is a slight residual temperature dependence below 200 K in the sudden rate. The slope of this portion gives the activation energy required to contract the O–Al–O angle to 89$^{\text{o}}$, the center of the dynamical distribution over a broad range of temperatures. The extreme low temperature limit of the sudden rate is ca. 10^{-5} s^{-1}, somewhat below the adiabatic limit of ca. 10^{-3} s^{-1}. This is because at extreme low temperatures, the adiabatic theory maintains the MEP barrier of 76.3 kJ mol^{-1}[B3LYP/6-311G(d,p)] while the only

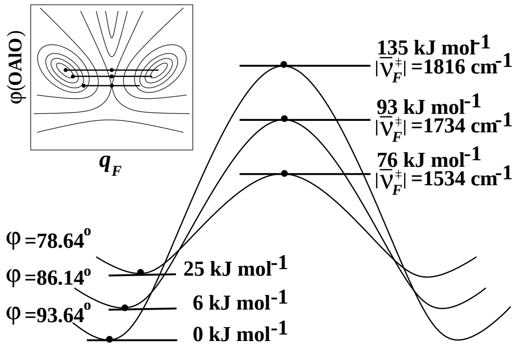

Figure 3. Schematic of three fixed–angle proton jump pathways, inset shows reaction path "curvature."

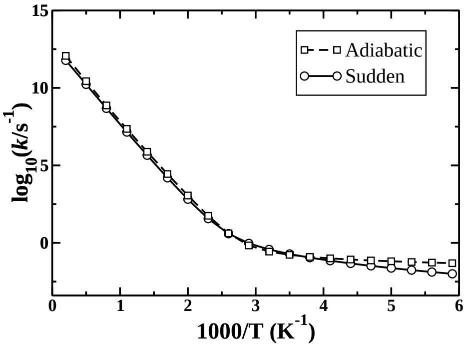

Figure 4. Arrhenius plot of rate coefficients from adiabatic and sudden approximations.

contributing fixed–angle pathway is at $\phi^r = 93.64^{\circ}$, with $\Delta E_0 = 135$ kJ mol^{-1}, and no classical activation for contraction of the O–Al–O angle. Forcing Arrhenius fits to the rate coefficients at the four temperatures used by Sarv *et. al.* yields apparent activation energies of 53.0 kJ mol^{-1} (adiabatic) and 55.8 kJ mol^{-1} (sudden) for the data represented in Fig. 4. These apparent activation energies remain in decent agreement with the 61 kJ mol^{-1} reported, but are not as good as those from the higher level electronic structure results. Although including long range interactions and higher levels of correlation would be too expensive with our current computer hardware, both would increase these values, and bring them into even better agreement with the experimental results.

Figure 4 also shows that in the temperature range 200 – 1000 K, which is most relevant to zeolite science, the two theories give essentially identical rates. This offers further justification for the use of our adiabatic theory despite its draconian approximations. It remains to be seen whether this holds true once we evaluate the consequences of neglecting barrier anharmonicity through comparisons with more rigorous quantum rate theories using chemical systems simpler to parameterize, or for proton transfer reactions involving adsorbate molecules in zeolites.

4. Conclusions

Using a reasonable cluster model of H–Y zeolite, we have shown that accurate and efficient calculation of the structural and vibrational characteristics of proton transfer reactions can be accomplished with density functional theory using the B3LYP functional and polarized basis sets of at least triple–ζ flexibility in the valence. Unfortunately, this method fails to predict quantitative energy differences, and we advocate using MP2 energies in a larger basis set augmented with MP4 energies in a more limited basis set to compute classical barrier heights. Even accounting for the effects of long–range interactions in an approximate fashion, we the barriers we calculate (97.1 kJ mol^{-1}) are significantly larger than those reported in the experimental literature (61 kJ mol^{-1}). By using our converged barrier heights and vibrational frequencies to parameterize the adiabatic limit of semiclassical transition state theory [SC–TST], we attibute the discrepancy to the neglect of tunneling in the interpretation of exerimental rate data. Addressing the neglect of so–called large curvature dynamics, we perform additional calculations to parameterize an angular sudden approximation to SC–TST. In the temperature range of interest, 200 to 1000 K, the two rate theories give nearly identical results, confirming our principal conclusion.

Acknowledgments

This work was supported by the National Science Foundation (CHE–9616019 and CTS–9734153), a Sloan Foundation Reasearch Fellowship (BR–3844), and a Camille Dreyfus Teacher–Scholar Award (TC–99–041). We thank Grateful Dead for their unwitting encouragement.

REFERENCES

1. J. Weitkamp, in *Catalysis and Adsorption by Zeolites*, edited by G. Olhmann, J. C. Vedrine, and P. A. Jacobs (Elsevier, Amsterdam, 1991), p. 21.
2. A. Corma, Chem. Rev. **95**, 559 (1995), and references therein.
3. J. Sauer, Chem. Rev. **98**, 199 (1989), and references therein.
4. R. A. van Santen and G. J. Kramer, Chem. Rev. **95**, 637 (1995), and references therein.
5. M. J. Rice, A. K. Chakraborty, and A. T. Bell, J. Phys. Chem. A **102**, 7498 (1998).
6. P. Sarv *et al.*, J. Phys. Chem. **99**, 13763 (1995).
7. J. T. Fermann, C. Blanco, and S. M. Auerbach, J. Chem. Phys. **112**, 6779 (2000).
8. J. Sauer, M. Sierka, and F. Haase, in *Transition State Modeling for Catalysis*, No. 721 in *ACS Symposium Series*, edited by D. G. Truhlar and K. Morokuma (ACS, Washington, 1999), Chap. 28, pp. 358–367.
9. M. Sierka and J. Sauer, J. Chem. Phys. **112**, 6983 (2000).
10. J. T. Fermann and S. M. Auerbach, J. Chem. Phys. **112**, 6787 (2000).
11. J. T. Fermann and S. M. Auerbach, 2001, in press.
12. J. A. Ryder, A. K. Chakraborty, and A. T. Bell, J. Phys. Chem. B **104**, 6998 (2000).
13. T. N. Truong, J. Phys. Chem. B **101**, 2750 (1997).
14. A. D. Becke, J. Chem. Phys. **98**, 5648 (1993).
15. C. Lee, W. Yang, and R. G. Parr, Phys. Rev. B **37**, 785 (1988).
16. C. Møller and M. S. Plesset, Phys. Rev. **46**, 618 (1934).
17. R. Krishnan and J. A. Pople, Int. J. Quantum Chem. **14**, 91 (1978).
18. R. Krishnan, M. J. Frisch, and J. A. Pople, J. Chem. Phys. **72**, 4244 (1980).
19. J. Sauer, C. M. Kolmel, J.-R. Hill, and R. Ahlrichs, Chem. Phys. Lett. **164**, 193 (1989).
20. M. Czjzek, H. Jobic, A. N. Fitch, and T. Vogt, J. Phys. Chem. **96**, 1535 (1992).
21. H. B. Schlegel, J. Comp. Chem. **3**, 214 (1982).
22. J. A. Pople, R. Krishnan, H. B. Schlegel, and J. S. Binkley, Int. J. Quantum Chem. Symp. **13**, 225 (1979).
23. N. C. Handy and H. F. Schaefer III, J. Chem. Phys. **81**, 5131 (1984).
24. M. Head-Gordon and T. Head-Gordon, Chem. Phys. Lett. **220**, 122 (1994).

25. B. G. Johnson and M. J. Frisch, J. Chem. Phys. **100**, 7429 (1994).
26. M. J. Frisch, *et al.*, GAUSSIAN98 (Revision A.3), Gaussian, Inc., Pittsburgh, PA, 1998.
27. C. L. Janssen, *et al.*, PSI 2.0.8, PSITECH, Inc., Watkinsville, GA 30677, U. S. A., 1995.
28. W. H. Miller, Faraday Discuss. Chem. Soc. **62**, 40 (1977).
29. R. Hernandez and W. H. Miller, Chem. Phys. Lett. **214**, 129 (1993).
30. W. H. Miller *et al.*, Chem. Phys. Lett. **172**, 62 (1990).
31. R. P. Bell, Trans. Faraday Soc. **55**, 1 (1959).
32. K. Raghavachari, G. W. Trucks, J. A. Pople, and M. Head-Gordon, Chem. Phys. Lett. **157**, 479 (1989).
33. G. E. Scuseria and T. J. Lee, J. Chem. Phys. **93**, 5851 (1990).
34. E. Merzbacher, *Quantum Mechanics* (John Wiley & Sons, New York, 1970).